Available online at www.sciencedirect.com
SCIENCE DIRECT®
Journal of Sound and Vibration 279 (2005) 1170–1180
JOURNAL OF SOUND AND VIBRATION
www.elsevier.com/locate/jsvi

Short Communication

Experimental verification of an algorithm for identification of linear time-varying systems

Kefu Liu*, Liyan Deng

Department of Mechanical Engineering, Lakehead University, 955 Oliver Road, Thunder Bay, Ont., Canada P7B 5E1

Received 20 June 2003; accepted 27 January 2004
Available online 7 October 2004

1. Introduction

In Ref. [1], a discrete-time state-space model is used to describe linear time-varying (LTV) systems subject to initial disturbance. The concept of pseudo-modal parameters is proposed to characterize dynamic properties of LTV systems. A subspace-based algorithm is developed to identify the model and the pseudo-modal parameters. The algorithm is verified by computer simulation. The goal of this study is to experimentally verify this algorithm. The study intends to address the following: (1) to study the applicability of the algorithm to a real system that may contain some imperfections such as a certain degree of nonlinearity and measurement noise, (2) to study the factors that affect implementation of the algorithm, and (3) to find solutions to some anticipated challenges such as selection of structural modes. An axially moving cantilever beam apparatus was built as a test-bed for this study. The experiment identification was carried out. This note reports the main findings of the study.

2. The identification algorithm

A state-space representation of an LTV system subject to initial disturbance is given by

$$\dot{\mathbf{x}}(t) = \mathbf{A}(t)\mathbf{x}(t), \mathbf{x}(0); \quad \mathbf{y}(t) = \mathbf{C}(t)\mathbf{x}(t), \tag{1}$$

*Corresponding author. Tel.: +1-807-343-8684.
E-mail address: kefu.liu@lakeheadu.ca (K. Liu).

0022-460X/$ - see front matter
doi:10.1016/j.jsv.2004.01.040

where $\mathbf{A}(t) \in R^{n_x \times n_x}$ and $\mathbf{C}(t) \in R^{n_y \times n_x}$ are referred to as the system matrix and the output matrix, respectively. The integer n_x represents the number of states or the order of model and n_y represents the number of outputs. The corresponding discrete-time state-space model of Eq. (1) is given by

$$\mathbf{x}(k+1) = \mathbf{G}(k+1,k)\mathbf{x}(k), \quad \mathbf{x}(0); \quad \mathbf{y}(k) = \mathbf{C}(k)\mathbf{x}(k), \quad k = 0, 1, \ldots, K-1, \tag{2}$$

where $\mathbf{G}(k+1,k)$ is referred to as the state transition matrix and K is the last moment of the time duration of interest. A similar transformation for the system is defined as

$$\bar{\mathbf{G}}(k+1,k) = \mathbf{T}(k+1)\mathbf{G}(k+1,k)\mathbf{T}^{-1}(k), \quad \bar{\mathbf{C}}(k) = \mathbf{C}(k)\mathbf{T}^{-1}(k), \tag{3}$$

where $\bar{\mathbf{G}}(k+1,k)$ and $\bar{\mathbf{C}}(k)$ are another realizations of the system. It is noted that, unlike the case of LTI systems, $\mathbf{G}(k+1,k)$ and $\bar{\mathbf{G}}(k+1,k)$ do not share the same eigenvalues because $\mathbf{T}(k+1) \neq \mathbf{T}(k)$ in general.

The pseudo-modal parameters are based on the eigenvalues of $\mathbf{G}(k+1,k)$. The eigendecomposition of $\mathbf{G}(k+1,k)$ is given as

$$\mathbf{G}(k+1,k) = \mathbf{V}(k)\mathbf{\Lambda}(k)\mathbf{V}^{-1}(k), \tag{4}$$

where $\mathbf{V}(k)$ and $\mathbf{\Lambda}(k)$ are the eigenvector matrix and eigenvalue matrix, respectively. Because the elements of $\mathbf{G}(k+1,k)$ are real, the complex eigenvalues occur in complex conjugate pairs. If the ith eigenvalue $\lambda_i(k)$ is complex, then the following expression can be employed:

$$\lambda_i(k) = \lambda_{i+1}^*(k) = \exp\left[-\zeta_i(k)\omega_i(k)\tau + \mathrm{j}\omega_i(k)\sqrt{1-\zeta_i^2(k)}\tau\right], \tag{5}$$

where $\omega_i(k) = 2\pi f_i(k)$ and $\zeta_i(k)$ are referred to as the ith pseudo-natural frequency (PNF) and pseudo-damping ratio (PDR) at the moment k, respectively, $\mathrm{j} = \sqrt{-1}$, and τ is the sampling time. The pseudo-modal parameters are defined in analogy to the definition of modal parameters for LTI systems.

The algorithm is based on an ensemble method that starts with forming a Hankel matrix using N sets of response data from N experiments:

$$\mathbf{H}(k) = \begin{bmatrix} \mathbf{y}^1(k) & \mathbf{y}^2(k) & \cdots & \mathbf{y}^N(k) \\ \mathbf{y}^1(k+1) & \mathbf{y}^2(k+1) & \cdots & \mathbf{y}^N(k+1) \\ \vdots & \vdots & \ddots & \vdots \\ \mathbf{y}^1(k+M-1) & \mathbf{y}^2(k+M-1) & \cdots & \mathbf{y}^N(k+M-1) \end{bmatrix}, \tag{6}$$

where $\mathbf{y}^j(k)$ denotes the response at the moment k from the jth experiment. Application of the Singular Value Decomposition (SVD) to $\mathbf{H}(k)$ allows to extract the range space of the observability matrix as

$$\bar{\mathbf{\Gamma}}(k) = \mathbf{\Gamma}(k)\mathbf{T}^{-1}(k) = \begin{bmatrix} \bar{\mathbf{C}}(k) \\ \bar{\mathbf{C}}(k+1)\bar{\mathbf{G}}(k+1,k) \\ \vdots \\ \bar{\mathbf{C}}(k+M-1)\bar{\mathbf{G}}(k+M-1,k) \end{bmatrix}. \tag{7}$$

To extract the matrix $\bar{\mathbf{G}}(k+1,k)$, a successive Hankel matrix $\mathbf{H}(k+1)$ is formed using the successive responses from the moment $k+1$ to the moment $k+M$.

The defined pseudo-modal parameters cannot be obtained from the eigenvalues of the matrix $\bar{\mathbf{G}}(k+1,k)$. In Ref. [1], a matrix is defined as

$$\tilde{\mathbf{G}}(k+1,k) = \mathbf{T}(k)\mathbf{G}(k+1,k)\mathbf{T}^{-1}(k). \tag{8}$$

Apparently the eigenvalues of $\tilde{\mathbf{G}}(k+1,k)$ are the same as those of $\mathbf{G}(k+1,k)$. In general, the matrix $\tilde{\mathbf{G}}(k+1,k)$ cannot be directly obtained from the extracted range space of the observability matrix. In Ref. [1], an approximate method was used to estimate $\tilde{\mathbf{G}}(k+1,k)$. Further studies have shown that this method is sensitive to measurement noise. In this study, an alternative approach is used. If $\bar{\mathbf{\Gamma}}_1(k)$ and $\bar{\mathbf{\Gamma}}_2(k)$ are formed by the first $M-1$ block rows and the last $M-1$ block rows of $\bar{\mathbf{\Gamma}}(k)$, respectively, the following relation exists:

$$\hat{\mathbf{G}}(k+1,k) = [\bar{\mathbf{\Gamma}}_1(k)]^{+}\bar{\mathbf{\Gamma}}_2(k) = \mathbf{T}(k)\mathbf{W}_1^{-1}\mathbf{W}_2\mathbf{G}(k+1,k)\mathbf{T}^{-1}(k), \tag{9}$$

where $(.)^{+}$ denotes the Moore–Penrose pseudo-inverse and

$$\mathbf{W}_1 = \sum_{i=0}^{M-2} \mathbf{G}^{\mathrm{T}}(k+i,k)\mathbf{C}^{\mathrm{T}}(k+i)\mathbf{C}(k+i)\mathbf{G}(k+i,k),$$

$$\mathbf{W}_2 = \sum_{i=0}^{M-2} \mathbf{G}^{\mathrm{T}}(k+i,k)\mathbf{C}^{\mathrm{T}}(k+i)\mathbf{C}(k+1+i)\mathbf{G}(k+1+i,k+1).$$

If $\mathbf{G}(k+i,k)$ and $\mathbf{C}(k+i)$ are close to $\mathbf{G}(k+1+i,k+1)$ and $\mathbf{C}(k+1+i)$, respectively, the matrix $\hat{\mathbf{G}}(k+1,k)$ can be used to approximate $\tilde{\mathbf{G}}(k+1,k)$. Complex conjugate pairs of the eigenvalues of $\hat{\mathbf{G}}(k+1,k)$ are used in Eq. (5) to find the approximate pseudo-natural frequency and pseudo-damping ratio at the moment k, respectively.

3. Experiment identification

Fig. 1 shows the experimental system. The beam is driven by a DC motor through a belt-pulley set and a pinion-rack set. The DC motor, manufactured by DUMORE, is a 12 V permanent magnet DC gearhead motor. The gear ratio is 13:1. The motor no-load speed is 180 rpm at 1.5 A. The transmission ratio of the belt-pulley set is 5.25:1. A potentiometer is attached to the pinion shaft to measure the angular position of the pinion shaft, and thus the linear position of the beam. The beam is made of 6061-T6 aluminum alloy. The cross-sectional dimension of the beam is 3.175 mm (thickness) × 50.8 mm (width). The length of the beam can vary from 0.66 to 1.09 m. The beam is guided through a slot made of Teflon. The clearance of the slot is properly chosen to emulate as close as possible a fixed end boundary condition. The lateral vibration of the beam is measured by a strain gauge sensor and two accelerometers (B & K 4393V). The strain gauge sensor is a full Wheatstone bridge and is located near the clamp with the beam fully retracted. Two accelerometers are placed at the tip and the middle of the beam, respectively. A 4-channel charge amplifier (B & K Nexus2692) is used to condition accelerometer signals. An unregulated DC power supplier and a servo linear amplifier were built in house. A Pentium III personal computer is used for control. The data acquisition (DAQ) board used is PCI-MIO-16E-4 by

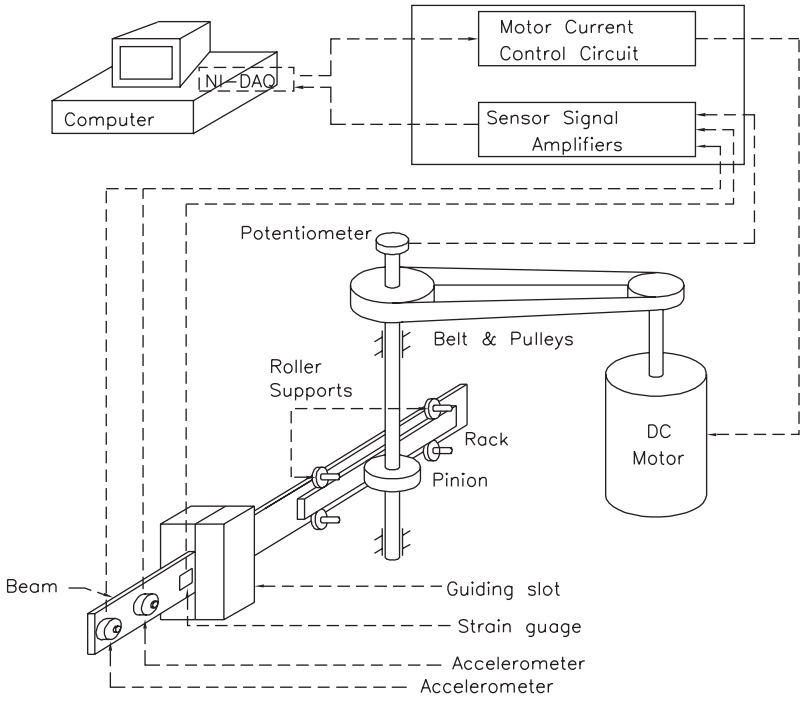

Fig. 1. Experimental system.

Table 1
Modal parameters of the first four modes for the fixed-length beams

Beam length	0.66 (m)		1.09 (m)	
Parameters	Experimental	Analytical	Experimental	Analytical
f_1 (Hz)/ζ_1	4.941/1.092E–2	5.958/NA	1.949/1.767E–2	2.185/NA
f_2 (Hz)/ζ_2	31.55/1.214E–2	37.34/NA	12.37/6.308E–3	13.69/NA
f_3 (Hz)/ζ_3	88.55/8.709E–3	104.6/NA	34.98/5.836E–3	38.33/NA
f_4 (Hz)/ζ_4	120.0/5.070E–4	204.8/NA	68.44/7.316E–3	75.12/NA

National Instruments. LabVIEW of National Instruments is used to interface with the DAQ board.

The details of the identification results can be found in Ref. [2]. In what follows, identification of the pseudo-natural frequencies is reported. As a preliminary study, the modal parameters of the fixed-length beams were determined. With the beam length fixed, free responses of the beam were produced by tapping the beam at various locations. The natural frequencies and damping ratios were estimated using a subspace-based identification method [3]. Table 1 gives a comparison of the experimental and analytical values. For the natural frequencies, the experimental values are lower than the analytical ones. This can be attributed to the fact that the beam does not have an

ideal fixed-end condition because of the clearance needed at the guiding slot. The damping ratios are low as it is only caused by the internal damping of the material and the air drag. The test also indicated that the modes higher than the fourth order are hardly excited out by an impact.

To generate an ensemble of free response data, it is important that the beam be engaged in the same axial motion for each experiment. Two motion scenarios were considered, namely, Scenario A: extension and Scenario B: retraction. Each motion scenario was conducted in a short duration denoted as fast motion and in a long duration denoted as slow motion, respectively. Therefore, four cases were considered, i.e., slow extension denoted as SA, fast extension denoted as FA, slow retraction denoted as SB, and fast retraction denoted as FB. A two-step control strategy was devised to command the motor motion [2]. A sampling frequency of 1000 samples per second was used. A LabVIEW program was written to execute the motor control and collect the sensor signals.

It is critical to generate a free response that is rich in the system dynamics and independent of the responses from other experiments. A great effort was made to ensure this. The beam was excited by tapping it at different locations with different intensities. The beam started to move after an impact was applied to ensure free response. After being acquired into the computer, the data were displayed and visually inspected first. All the data used for identification were forced to be zero-mean. Numerous experiments were conducted. In what follows, 40 experiments were used in each of four cases, i.e., $N = 40$.

After a Hankel matrix is formed using N sets of responses from k to $k + M - 1$, an SVD is conducted,

$$\mathbf{H}(k) = \mathbf{U}(k)\Sigma(k)\mathbf{V}^{\mathrm{T}}(k), \tag{10}$$

where $\mathbf{U}(k) \in R^{n_y M \times n_y M}$ and $\mathbf{V}(k) \in R^{N \times N}$ are left and right orthogonal singular vector matrices, respectively, and $\Sigma(k) \in R^{n_y M \times N}$ is diagonal and contains singular values arranged in a descending order. After a model order n_x is chosen, the first n_x columns of $\mathbf{U}(k)$ are used as the range space of the observability matrix. In the case of time-invariant systems, the magnitudes of singular values are used to determine a proper order for an identification model. In the case of time-varying systems, singular values vary from moment to moment. The study showed that the responses in the beginning of motion contain more modes than those in the later period of motion. The responses from the fast motion are richer in modal information than those from the slow motion. Such behaviors are due to the nature of free responses. The experiments also revealed that, when the beam is retracting, the measured signals appear to be diverging. As a result, the responses under retraction sustain a longer period and contain more modes than those under extension. This can be explained by the energetics of translating media with a varying length. In Ref. [4], it is proved that the energy of vibration decreases and increases monotonically during extension and retraction, respectively.

When the eigendecomposition is conducted on the identified matrix $\hat{\mathbf{G}}(k+1,k)$, real eigenvalues may appear due to system nonlinearity and/or measurement noise. As the pseudo-modal parameters are defined using pairs of complex eigenvalues, real eigenvalues are discarded. If there are n_r real eigenvalues, the number of identified PNFs is $n_f = (n_x - n_r)/2$.

It is necessary to overparameterize a model in order to capture the dynamics of the system. As a result of overparameterization, an identified transition matrix $\hat{\mathbf{G}}(k+1,k)$ contains two types of modes: structural modes and computational modes. How to distinguish the structural modes from

the computational modes poses a challenge for time-varying systems. For time-invariant systems, several methods are available such as the balanced realization technique [5] and the mode singular value [6]. These methods cannot be directly applied to time-varying systems. In this study, the problem is treated as how to group the values $f_i(k)$, i.e., what is the next $f_i(k+1)$? A natural choice of grouping is to sort all the identified PNFs at each moment according to their magnitudes. Fig. 2 shows the first four PNFs sorted in an ascending order. They were identified using the responses of case FB with the model order of $n_x = 14$ and the block row number of $M = 140$.

It can be seen that the first group of the values belongs to the first PNF. The second group of the values belongs to the second PNF for almost the entire duration of motion except a short period towards the end. The third group of values start to represent the third PNF. However, around the middle of the motion duration, the values oscillate between the second PNF and the third PNF. The fourth group of values is even less sensible. Sorting the identified PNFs according to their magnitudes at each moment fails because of the presence of the spurious frequencies associated with the computational modes. In the beginning of motion, the structural modes dominate the signals and the spurious frequencies are likely to be large values because the noise tends to be of high frequencies. Towards the end of motion, the higher structural modes become less dominant in the signals and more spurious frequencies appear in the lower frequency region.

In this study, a method of grouping the identified PNFs is developed. The method is based on an assumption that a system PNF does not change significantly in a short time. To explain the method, the following notations are defined: $f_i(k)$ denotes the ith identified PNF sorted in an

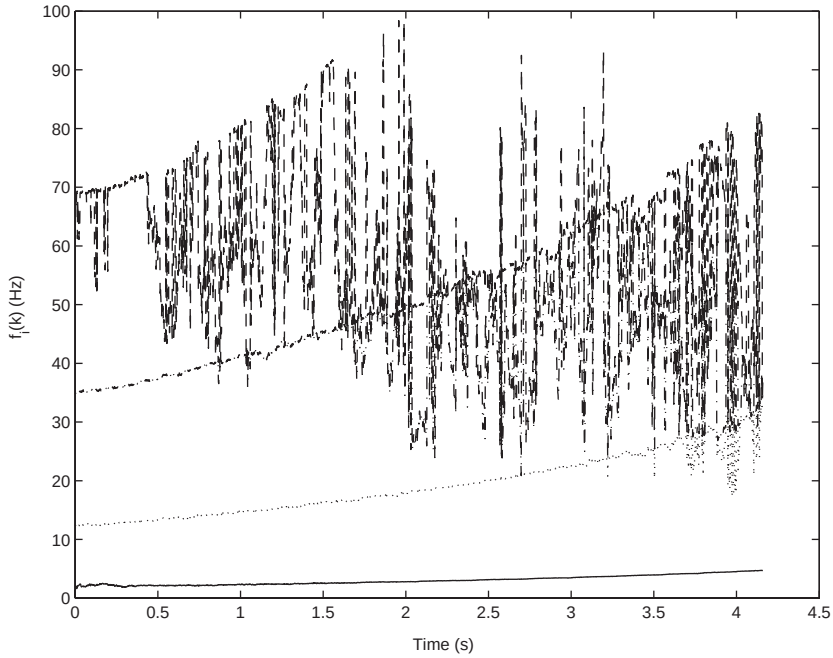

Fig. 2. Sorted PNFs from scenario FB: —, $f_1(k)$; ……, $f_2(k)$; -.-.-., $f_3(k)$; - - -, $f_4(k)$.

ascending order; $f_i^s(k)$ the ith selected PNF; and $f_i^a(k)$ a moving mean of the selected PNFs from $k - M_1 + 1$ to k, i.e.,

$$f_i^a(k) = \text{mean}[f_i^s(k - M_1 + 1) : f_i^s(k)] = \frac{1}{M_1} \sum_{j=k-M_1+1}^{k} f_i^s(j), \tag{11}$$

where M_1 is a prescribed number. With $f_i^a(k)$, the ith selected PNF at the next moment $k + 1$ or $f_i^s(k + 1)$ is selected from $f_i(k + 1)$, $i = 1, 2, \ldots, n_f$, to be the one that is closest to $f_i^a(k)$. To start the process of selection, let $f_i^a(0) = f_i(0)$, i.e., the values ranked by magnitude at the first moment are chosen to be the mean values. For $k < M_1 - 1$, k is used as M_1, i.e., the mean values are calculated using the selected values available.

Fig. 3 shows the first four PNFs selected from the results partly presented in Fig. 2. The selected results were obtained using $M_1 = 10$. From the figure, it can be seen that the first three sets of the selected values represent the first, second, and third PNFs, respectively. The fourth set of the selected values represents the fourth natural frequency in the beginning and becomes very irregular towards the end. This indicates that the first three PNFs were successfully identified while the fourth PNF was not completely identified for the entire duration of motion.

Fig. 4 shows the first three PNFs identified using the responses of case FA and sorted by magnitude. The identification was conducted with the model order of $n_x = 14$ and the block row number of $M = 140$. It can be seen that the second and third sets of the values fluctuate significantly. Fig. 5 shows the first three groups of the selected values. The selected results were obtained using $M_1 = 10$. It can be seen that the first three PNFs were successfully found except

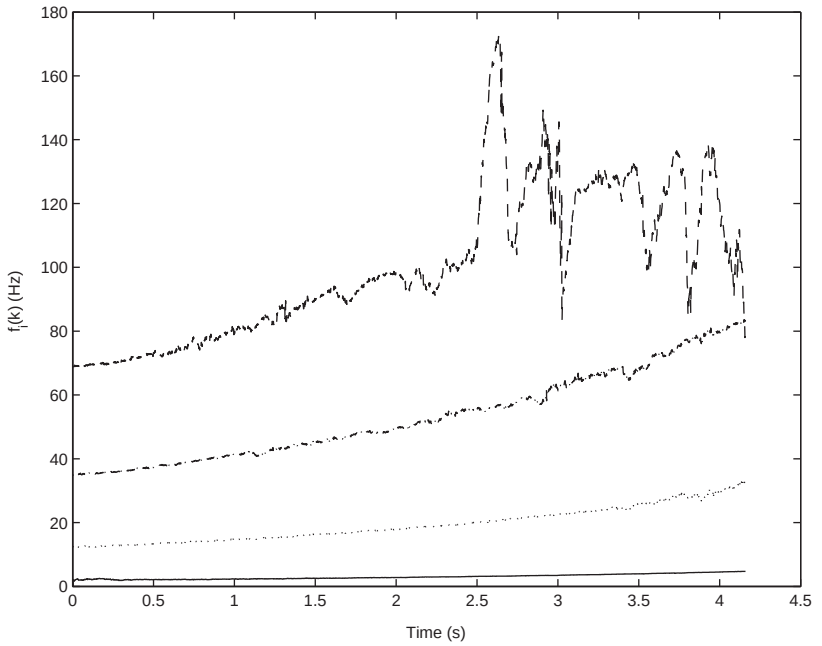

Fig. 3. Selected PNFs from scenario FB: —, $f_1^s(k)$; ……, $f_2^s(k)$; -.-.-., $f_3^s(k)$; - - -, $f_4^s(k)$.

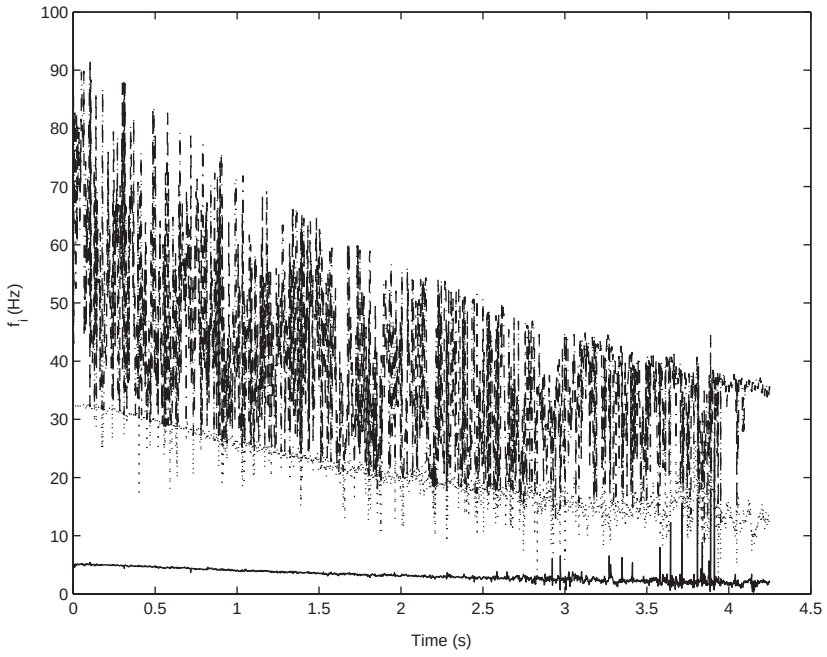

Fig. 4. Sorted PNFs from scenario FA: —, $f_1(k)$; ……, $f_2(k)$; -.-.-., $f_3(k)$.

that towards the end of motion, the results become less satisfactory. The above results indicate that the proposed method can properly group the identified PNFs. Therefore, the method is used in the following discussion.

With $f_i^s(k)$, a quantity that measures variation of the selected values is defined as

$$\sigma_i = \frac{1}{K}\sum_{i=0}^{K-1}\sigma_i(k), \quad \sigma_i(k) = \mathrm{std}[f_i^s(k-M_2+1) : f_i^s(k)], \tag{12}$$

where $\mathrm{std}[f_i^s(k-M_2+1) : f_i^s(k)]$ represents a moving standard deviation of the ith selected PNF from $k-M_2+1$ to k and M_2 is a prescribed number. It is reasonable to assert that if the ith selected PNF has a small value of σ_i, it is more likely to represent a structural mode. In addition, the mean PNFs in the beginning and the end of motion are defined as

$$f_{ib}^a = f_i^a(M_1-1) \quad \text{and} \quad f_{ie}^a = f_i^a(K-1),$$

respectively. Comparison of the values of f_{ib}^a and f_{ie}^a with the corresponding values presented in Table 1 reveals whether the identified PNFs follow the overall varying trends.

Table 2 summarizes the identification results using the responses of case FA with $M = 50$. From the table, one can see that with $n_x = 6$, identification of the first PNF is possible and with $n_x = 16$, identification of the first three PNFs is possible for the entire duration of motion. The results with $M = 100$ are given in Table 3. With an increase of the block row number M, the first two groups of the selected values become more consistent, indicated by smaller mean standard deviations. The results for the third group of the selected values seem difficult to explain at first

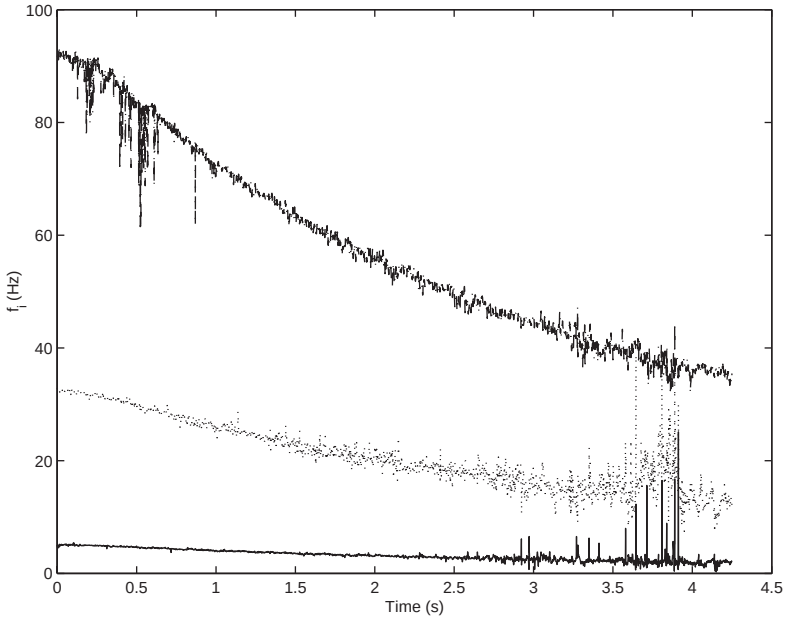

Fig. 5. Selected PNFs from scenario FA: —, $f_1^s(k)$; ……, $f_2^s(k)$; -.-.-., $f_3^s(k)$.

Table 2
The identification results for FA. $M = 50$, $M_1 = M_2 = 20$

n_x	f_{1b}^a/f_{1e}^a (Hz)	σ_1	f_{2b}^a/f_{2e}^a (Hz)	σ_2	f_{3b}^a/f_{3e}^a (Hz)	σ_3	f_{4b}^a/f_{4e}^a (Hz)	σ_4
6	5.292/2.940	0.6451	NA	NA	NA	NA	NA	NA
10	5.153/2.118	0.4862	32.30/35.57	1.608	87.35/11.54	8.003	NA	NA
14	4.936/1.845	0.3397	32.49/12.77	1.264	91.68/34.79	2.996	78.81/62.37	18.71
16	4.824/1.871	0.3470	32.49/12.60	1.127	91.97/34.45	1.082	89.16/65.43	10.29

glance. The identified values for f_{3e}^a are sensible when $n_x \geqslant 10$. However, the values for f_{3b}^a are inconsistent, for example, in the cases of $n_x = 14$ and $n_x = 16$. Considering f_{4b}^a in the case of $n_x = 16$, one can see that a more proper value was used as the fourth group of the selected values. This indicates a limitation of the proposed selection method as it starts with the values sorted by magnitude at the first moment. In this case, the third smallest value is spurious. This problem can be overcome if the selection starts with a set of known values, such as those given in Table 1.

Table 4 lists the identification results using the responses of case FB. With $n_x \geqslant 14$, the first two PNFs were identified. With $n_x \geqslant 16$, the first three PNFs were identified. Identification with various values of the block number M was conducted. The results indicate that a proper selection of the block number M is important. In general, a larger M implies that the extracted subspace is valid over a longer time interval, thus contains richer modal information and yields more consistent results.

The identification results using the responses of case SA were not satisfactory. The algorithm was able to identify the first PNF for the duration of motion. For the second and third PNFs, the

Table 3
The identification results for FA. $M = 100$, $M_1 = M_2 = 20$

n_x	f^a_{1b}/f^a_{1e} (Hz)	σ_1	f^a_{2b}/f^a_{2e} (Hz)	σ_2	f^a_{3b}/f^a_{3e} (Hz)	σ_3	f^a_{4b}/f^a_{4e} (Hz)	σ_4
6	4.980/2.378	0.0592	32.32/27.84	3.230	NA	NA	NA	NA
10	4.953/2.028	0.0585	32.23/12.21	0.9368	80.95/35.55	7.938	NA	NA
14	5.117/2.006	0.0666	32.28/12.51	0.5989	91.20/35.01	1.295	86.60/63.62	8.047
16	5.125/2.007	0.0675	32.37/12.43	0.5420	55.08/35.19	2.151	89.99/64.66	7.433

Table 4
The identification results for FB. $M = 100$, $M_1 = M_2 = 20$

n_x	f^a_{1b}/f^a_{1e} (Hz)	σ_1	f^a_{2b}/f^a_{2e} (Hz)	σ_2	f^a_{3b}/f^a_{3e} (Hz)	σ_3	f^a_{4b}/f^a_{4e} (Hz)	σ_4
6	7.626/29.44	0.5394	33.57/4.691	1.138	NA	NA	NA	NA
10	12.20/31.61	0.3662	34.75/56.59	0.7541	68.41/4.692	2.841	108.3/79.88	7.312
14	2.381/31.26	0.2519	12.44/83.94	0.7411	34.94/48.43	5.282	68.84/4.740	3.067
16	2.363/4.734	0.0483	12.45/31.80	0.1956	35.02/84.21	0.5314	68.84/68.41	4.085

algorithm was able to identify them in the beginning of motion and failed to do so towards the end of motion. This is due to the fact that high modes become too weak to be detected when the duration of motion is long. The identification results using the responses of case SB were better than those using the responses of case SA and worse than those using the responses of case FB. Identification using different numbers of experiments was also conducted. The study indicates that it is possible to identify the first three PNFs using fewer number of experiments. When the number of experiments is small, the quality of the response from each experiment becomes more critical. A response with a high quality should be rich in modal information and independent of the other responses. More studies were carried out such as the use of one or two outputs, the use of different number M_1 in selection of the structural PNFs, etc. Due to the limited paper length, they are not reported here.

4. Conclusions

The following conclusions can be drawn from the study: The algorithm is capable of identifying the first three pseudo-natural frequencies. The study has indicated that the newly defined approximate transition matrix is less sensitive to measurement noise than the one defined in Ref. [1]. A method to select the structural pseudo-natural frequencies from the identified values has been developed. The identification results have indicated that the proposed method is able to properly group the structural frequencies. The study has revealed that the proper implementation of the algorithm depends on several factors. To generate an ensemble of free responses from multiple experiments, the beam must be in the same axial motion for each experiment. The impact used in each experiment must be distinct in order to produce responses independent of each other. The model must be properly overparameterized to capture all the excited structural modes. The

measured responses must be detrended to have zero-mean. The larger block row number in general gives a better result. The more the experiments are used in forming the data matrix, the more consistent the identification results become.

The experimental study has also confirmed some interesting behaviors of the axially moving cantilever beams. For example the energy of vibration decreases and increases monotonically during extension and retraction, respectively. Such a behavior has an impact on identification. It has been observed that the responses under retraction motion are richer in modal information and sustain a longer period than those under extension motion. Therefore more modes can be identified using the responses under retraction motion than using those under extension motion.

The study has revealed some limitations of the algorithm. As free responses decay quickly, the quality of identification deteriorates with an increase of time if the system response is not persistently exciting as the case of an axial extension. The results of identification of the pseudo-damping ratios are not acceptable mainly due to two reasons. First, the eigenvalues of the matrix $\hat{\mathbf{G}}(k+1,k)$ defined in Eq. (9) do not give a close approximation to the pseudo-damping ratios. Determination of the exact matrix $\tilde{\mathbf{G}}(k+1,k)$ defined in Eq. (8) by the subspace extraction is not possible. Second, because the damping level of the system is low and varying, the identified damping ratios are very sensitive to measurement noise. The study has been limited to two motion scenarios: extension and retraction. The future study will test the algorithm against more complicated motion patterns such as parabolic and periodic root motions.

References

[1] K. Liu, Identification of linear time-varying systems, *Journal of Sound and Vibration* 204 (1997) 487–500.

[2] L. Deng, Modeling and Identification of an Axially-moving Cantilever Beam, MSc Engineering Thesis, Lakehead University, Thunder Bay, ON, 2002.

[3] K. Liu, Modal parameter estimation using the state space method, *Journal of Sound and Vibration* 197 (1996) 387–402.

[4] W.D. Zhu, J. Ni, Energetics and stability of translating media with an arbitrarily varying length, *Journal of Vibration and Acoustics* 122 (2000) 295–304.

[5] K. Liu, D.W. Miller, Time domain state space identification of structural systems, *Journal of Dynamic Systems, Measurement, and Control* 117 (1995) 608–618.

[6] J. Juang, *Applied System Identification*, Prentice-Hall, Englewood Cliffs, NJ, 1994.